Numerische Mathematik manuscript No.
(will be inserted by the editor)

Why the MUSCL-Hancock scheme is L^1-stable

Christophe BERTHON

[1] MAB, UMR 5466, Université Bordeaux I, 351 cours de la libération, 33400 Talence, France.
[2] INRIA Futurs, projet ScAlApplix, Domaine de Voluceau-Rocquencourt, B.P. 105, 78153 Le Chesnay Cedex France.

Summary The finite volume methods are one of the most popular numerical procedure to approximate the weak solutions of hyperbolic systems of conservation laws. They are developed in the framework of first-order numerical schemes. Several approaches are proposed to increase the order of accuracy. The van Leer methods are interesting ways. One of them, namely the MUSCL-Hancock scheme, is full time and space second-order accuracy. In the present work, we exhibit relevant conditions to ensure the L^1-stability of the method. A CFL like condition is established, and a suitable limitation procedure for the gradient reconstruction is developed in order to satisfy the stability criterion. In addition, we show that the conservative variables are not useful within the gradient reconstruction and the procedure is extended in the framework of the primitive variables. Numerical experiments are performed to show the interest and the robustness of the method.

Key words Hyperbolic systems, Finite volume schemes, MUSCL-Hancock method, L^1-stability

1 Introduction

In the present work, we discuss the numerical approximation for solving hyperbolic system of conservation laws such as the well-known Euler equations. We propose to consider finite volume methods with time and space second-order of accuracy. During the twenty last years,

the problem of increasing the order of accuracy for solving hyperbolic system has been a very active research topic. Actually, one of the most popular second-order scheme has been introduced by van Leer [16]; namely the MUSCL scheme. It is a finite volume method where the flux approximation is second-order accurate. This scheme is considered and extended in a lot of applications, for instance see Collela [6], Durlofsky-Engquist-Osher [9], Sander-Wieser [23] and references therein (see also Toro [24] and Godlewski-Raviart [11]).

Since the scheme is used to perform very difficult numerical flow simulations, the robustness turns out to be central. Several works are devoted to such an analysis. The first ones are proposed by Khobalatte-Perthame [15], Perthame-Qiu [22] when the authors enforce the L^1-stability as soon as the gradient reconstruction satisfies a conservation argument. Next, in Berthon [2], the author shows how preserve the L^1-stability but for no conservation assumption in the gradient reconstruction. Moreover, second-order discrete entropy inequalities are given in [2].

In van Leer [17], a variant of the MUSCL scheme is introduced; namely the MUSCL-Hancock method. This scheme is full time and space second-order accurate. It differs from the other MUSCL variants [15, 16, 22, 24] in its second-order time of accuracy. Indeed, the time accuracy rises when considering a step based on a central-like scheme (see Nessyahu-Tadmor [20] or Bianco-Puppo-Russo [4]). In the present work, we propose to consider the MUSCL-Hancock scheme for a stability and robustness analysis.

This paper is organized as follows. In the following section, we introduce the main notations and we describe the MUSCL-Hancock method. Next, in the third section, we analyze the robustness of the scheme under consideration. Arguing a relevant limitation procedure to define the gradient reconstruction, we establish the L^1-stability of the scheme. The stability result involves a more restrictive CFL condition than usually meet. This may imply several difficulties from a practical point of view. In the next section, we propose a time variant of the MUSCL-Hancock scheme which makes easy (more standard) the time CFL restriction. At this level of the paper, the piecewise-linear reconstruction is based on the conservative variables. We propose to extend the above analysis within the framework of a gradient reconstruction based on relevant non-conservative variables. To conclude the paper, the last section is devoted to the numerical experiments. They are performed within classical Euler equations. The numerical tests show the interest and the robustness of the method.

2 The MUSCL-Hancock method

We consider hyperbolic systems of conservation laws in the form

$$\partial_t \mathbf{w} + \partial_x \mathbf{f}(\mathbf{w}) = 0, \quad t >, \ x \in \mathbb{R}, \tag{1}$$

where $\mathbf{w}(x,t)$ is the vector state solution made of N components, and $\mathbf{f}$ denotes the flux function. The state vector $\mathbf{w}$ belongs to a convex set Ω, assumed to be invariant by the flow. In general, the invariance of Ω is dictated by physical properties (an example will be given in the section 5 devoted to the numerical experiments). Let us emphasize that the present analysis will apply to some specific systems (for instance gas dynamics) because of an invariance assumption. Indeed, in the sequel we need the invariance of Ω under the Riemann problem. Such an assumption turns out to be restrictive even if the gas dynamics equations enter the present framework.

From now on, let us note that an additional assumption will be imposed to the set Ω. In fact, we will enforce that the invariance by the flow of Ω implies the numerical L^1-stability. For instance, the phase space Ω associated with the standard Euler equations satisfies such a property (see Godlewski-Raviart [11]).

Now, we turn considering the numerical approximation of solutions of (1). The MUSCL-Hancock method (see van Leer [17] but also Toro [24]) is considered in the present work. It achieves a second-order extension of a first-order finite volume scheme. It has three distinct steps: The data reconstruction, The evolution, The Riemann problem.

The data reconstruction. In this step, we introduce a linear piecewise function to approximate the solutions of (1), namely

$$\mathbf{w}^n(x) = \mathbf{w}_i^n + \sigma_i(x - x_i), \quad x \in (x_{i-\frac{1}{2}}, x_{i+\frac{1}{2}}),$$

where $(x_i)_{i\in\mathbb{Z}}$ denotes the mesh nodes. We have set $x_{i+\frac{1}{2}} = x_i + (x_{i+1} - x_i)/2$. For the sake of simplicity in the present work, we will assume that the mesh is uniform with the size Δx. The value σ_i defines a suitable slope of the linear function set in the cell $(x_{i-\frac{1}{2}}, x_{i+\frac{1}{2}})$. Concerning the choice of σ_i, the reader is referred to [10,11,18,24].

We consider the inner approximation in the cell $(x_{i-\frac{1}{2}}, x_{i+\frac{1}{2}})$, located at $x = x_{i\pm\frac{1}{2}}$. These approximations are denoted $\mathbf{w}_i^{n,\pm}$ and are defined as follows:

$$\mathbf{w}_i^{n,\pm} = \mathbf{w}_i^n \pm \frac{\Delta x}{2}\sigma_i. \tag{2}$$

To conclude the first step, let us note that we have assumed a reconstruction based on the conservative variables. Some authors propose to consider other variables to make the reconstruction. Latter on, we will discuss about the case of *non-conservative* piecewise linear reconstruction.

The evolution. The inner approximations are evolved by a time $\Delta t/2$ as follows:

$$\mathbf{w}_i^{n+\frac{1}{2},\pm} = \mathbf{w}_i^{n,\pm} - \frac{\Delta t}{2\Delta x}\left(\mathbf{f}(\mathbf{w}_i^{n,+}) - \mathbf{f}(\mathbf{w}_i^{n,-})\right). \tag{3}$$

The Riemann problem. The updated approximate solution at time t^{n+1} is given by

$$\mathbf{w}_i^{n+1} = \mathbf{w}_i^{n} - \frac{\Delta t}{\Delta x}\left(\mathbf{f}_{i+\frac{1}{2}} - \mathbf{f}_{i-\frac{1}{2}}\right), \tag{4}$$

where $\mathbf{f}_{i+\frac{1}{2}}$ denotes the numerical flux function. Following the standard Godunov scheme, the numerical flux function reads:

$$\mathbf{f}_{i+\frac{1}{2}} = \mathbf{f}(\omega_e(0; \mathbf{w}_i^{n+\frac{1}{2},+}, \mathbf{w}_{i+1}^{n+\frac{1}{2},-})),$$

with $\mathbf{f}$ the exact flux function while $\omega_e(., \mathbf{w}_L, \mathbf{w}_R)$ denotes the exact solution of the Riemann problem for (1) with the initial data $\mathbf{w}_0(x) = \mathbf{w}_L$ if $x < 0$ and $\mathbf{w}_R$ otherwise. In fact, one extends this step to more general first-order numerical flux function:

$$\mathbf{f}_{i+\frac{1}{2}} = \mathbf{f}(\mathbf{w}_i^{n+\frac{1}{2},+}, \mathbf{w}_{i+1}^{n+\frac{1}{2},-}), \tag{5}$$

where $\mathbf{f}(\mathbf{w}_L, \mathbf{w}_R)$ can be the Godunov numerical flux function but also the HLL, relaxation, Roe, etc, numerical flux function.

Concerning this time and space second-order accurate scheme, we note that no CFL restriction is actually established. Authors proposed several choice (for instance see van Leer [17] or Toro [24]) but it must be used with *caution*. In the present work, we detail a relevant CFL restriction to enforce the L^1-stability. To access such an issue, we will introduce a relevant gradient reconstruction limitation in the first step (2).

In the sequel, we will consider systems (1), set over Ω, such that the L^1-stability of schemes is implied by the numerical invariance of Ω: $\mathbf{w}_i^{n+1} \in \Omega$ whenever $\mathbf{w}_i^n \in \Omega$ for all $i \in \mathbb{Z}$. Let us remark that this assumption does not turn out to be very restrictive since many physical hyperbolic systems satisfy such hypothesis (for instance, see

[3,11] for the Euler equations and several derivation, but also see [8] in the framework of the radiative transfer).

To conclude the presentation of the MUSCL-Hancock method, we add an assumption concerning the numerical flux function $\mathbf{f}(\mathbf{w}_L, \mathbf{w}_R)$ used in (4). When considering the associated first-order scheme:

$$\mathbf{w}_i^{n+1} = \mathbf{w}_i^n + \frac{\Delta t}{\Delta x}\left(\mathbf{f}(\mathbf{w}_i^n, \mathbf{w}_{i+1}^n) - \mathbf{f}(\mathbf{w}_{i-1}^n, \mathbf{w}_i^n)\right), \tag{6}$$

the first-order approximate solution must be L^1-stable. Several first-order numerical flux functions satisfy such a property as long as the time increment Δt satisfies the following first-order CFL condition:

$$\frac{\Delta t}{\Delta x}\max_{i\in\mathbb{Z}}|\lambda(\mathbf{w}_i^n, \mathbf{w}_{i+1}^n)| \leq \frac{1}{2}, \quad \forall i \in \mathbb{Z}. \tag{7}$$

With some abuse in the notations, $\lambda(\mathbf{w}_i^n, \mathbf{w}_{i+1}^n)$ denotes the numerical eigenvalues of the Jacobian matrix associated with the flux function $\mathbf{f}$ and evaluated at the cell interface $x_{i+\frac{1}{2}}$. In the sequel, $\lambda_e(\mathbf{w}_L, \mathbf{w}_R)$ will denote the exact eigenvalues of the system (1).

Put in other words, the numerical flux function, introduced in (4), must ensure the invariance of Ω when considering the first-order scheme (6)-(7). Many finite volume methods satisfy such a property. For instance, the well-known Godunov flux function can be considered (as proposed by van Leer [17]) but also the Lax-Friedrichs or the kinetic or the relaxation schemes can be considered (see Bouchut [5]).

In addition, let us note from now on that we do not impose that the numerical flux function, considered in (4), is based on a Riemann solver (see Harten-Lax-van Leer [12]).

3 Stability results

In this section, we establish the main stability result enforcing the numerical invariance of Ω. We propose to detail a new second-order CFL condition and a relevant gradient reconstruction to ensure that $\mathbf{w}_i^{n+1} \in \Omega$ whenever $\mathbf{w}_i^n \in \Omega$ for all $i \in \mathbb{Z}$, where the sequence $(\mathbf{w}_i^{n+1})_{i\in\mathbb{Z}}$ is evaluated by the MUSCL-Hancock scheme (2)-(3)-(4)-(5). To access such an issue, we impose the numerical invariance of Ω at the end of each step of the method.

Concerning the first step, we have to consider a gradient reconstruction such that $\mathbf{w}_i^{n,\pm}$, defined by (2), belongs to Ω. Currently, we do not impose a specific limiter to evaluate σ_i since it depend on the system (1) and the admissible state space Ω. For instance, the reader

is referred to [2,10,11,18,24] where examples are given in the framework of Euler equations. In the sequel, we assume $\mathbf{w}_i^{n,\pm} \in \Omega$. Relevant choice of gradient reconstruction procedures will be specified in the section 5 devoted to the numerical experiments.

During the second step, the inner approximations are evolved in time to get $\mathbf{w}_i^{n+\frac{1}{2},\pm}$ defined by (3). In the following result, we establish a suitable CFL condition and a slope limitation to enforce $\mathbf{w}_i^{n+\frac{1}{2},\pm}$ to be in Ω.

Lemma 1 *Assume that $\mathbf{w}_i^n \in \Omega$ for all $i \in \mathbb{Z}$. Let us define $\mathbf{w}_i^{\star,\pm}$ as follows:*

$$\frac{1}{4}\mathbf{w}_i^{n,-} + \frac{1}{2}\mathbf{w}_i^{\star,\pm} + \frac{1}{4}\mathbf{w}_i^{n,+} = \mathbf{w}_i^{n,\pm}, \tag{8}$$

where $\mathbf{w}_i^{n,\pm}$ are defined by (2). Assume that

$$\mathbf{w}_i^{n,\pm} \in \Omega \quad \text{and} \quad \mathbf{w}_i^{\star,\pm} \in \Omega. \tag{9}$$

Consider the following CFL restriction:

$$\frac{\Delta t/2}{\Delta x/4} \max_{i\in\mathbb{Z}} \Big(|\lambda_e(\mathbf{w}_i^{n,-}, \mathbf{w}_i^{\star,\pm}|), |\lambda_e(\mathbf{w}_i^{\star,\pm}, \mathbf{w}_i^{n,+}|) \Big) \leq \frac{1}{2}. \tag{10}$$

Then, the invariance of Ω is satisfied at the end of the first step of the MUSCL-Hancock scheme: $\mathbf{w}_i^{n+\frac{1}{2},\pm} \in \Omega$, where $\mathbf{w}_i^{n+\frac{1}{2},\pm}$ is defined by (3).

From now on, let us note that the limitation imposed to the inner approximations $\mathbf{w}_i^{n,\pm}$ is standard. Indeed, if $\mathbf{w}_i^{n,\pm}$ does not belong to Ω, the flux evaluation at these states, in general, are not defined. The actual novelty is the limitation imposed on the intermediate states $\mathbf{w}_i^{\star,\pm}$. In fact, this additional limitation is not too restrictive (see section 5) and the accuracy of the scheme is preserved.

Let us remark that introducing intermediate states $\mathbf{w}_i^{\star,\pm}$ follows an idea proposed in [2].

Proof For the sake of simplicity, we just establish that $\mathbf{w}_i^{n+\frac{1}{2},+}$ is in Ω. The proof turns out to be similar to establish $\mathbf{w}_i^{n+\frac{1}{2},-} \in \Omega$ and thus it will not be detailed here.

First, we propose to interpret the evolution step (3) as a Riemann solver.

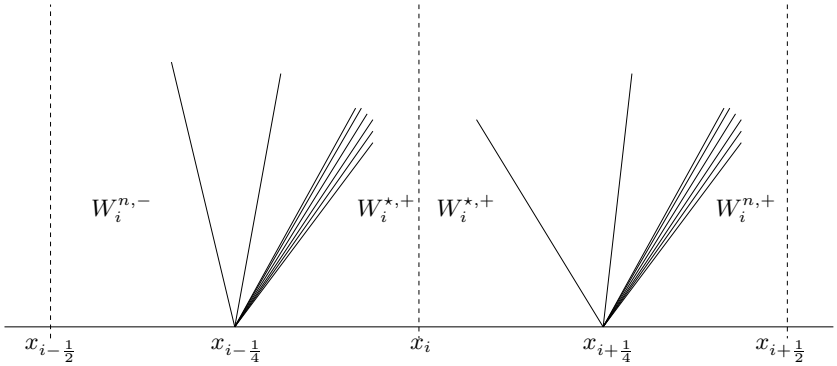

Fig. 1. Riemann solver interpretation of the evolution step (3).

Over the cell $(x_{i-\frac{1}{2}}, x_{i+\frac{1}{2}})$, we introduce $\mathbf{w}^h(x,t) : \mathbb{R} \times \mathbb{R}_+ \to \Omega$. With $t \in (0, \Delta t/2)$, the function $\mathbf{w}^h(x,t)$ is the weak solution of the Cauchy problem for (1) using the following initial data (see figure 1):

$$\mathbf{w}^h(x,0) = \begin{cases} \mathbf{w}_i^{n,-}, & \text{if } x \in (x_{i-\frac{1}{2}}, x_{i-\frac{1}{4}}), \\ \mathbf{w}_i^{\star,+}, & \text{if } x \in (x_{i-\frac{1}{4}}, x_{i+\frac{1}{4}}), \\ \mathbf{w}_i^{n,+}, & \text{if } x \in (x_{i+\frac{1}{4}}, x_{i+\frac{1}{2}}). \end{cases}$$

Under the CFL like condition (10), the solution $\mathbf{w}^h$ at time $\frac{\Delta t}{2}$ is made of the juxtaposition of solutions of non-interacting Riemann problems arising at the cell interfaces $x_{i\pm\frac{1}{4}}$.

Now, the projection of $\mathbf{w}^h(x, \frac{\Delta t}{2})$ on piecewise-constant functions gives

$$\mathbf{w}_i^{n+\frac{1}{2},+} = \frac{1}{\Delta x} \int_{x_{i-\frac{1}{2}}}^{x_{i+\frac{1}{2}}} \mathbf{w}^h(x, \frac{\Delta t}{2})\ dx. \tag{11}$$

Employing the formalism introduced by Harten-Lax-van Leer [12], we rewrite the latter equation as follows:

$$\mathbf{w}_i^{n+\frac{1}{2},+} = \frac{1}{4}\Big(\bar{\mathbf{w}}_L(\mathbf{w}_i^{n,-}, \mathbf{w}_i^{\star,+}) + \bar{\mathbf{w}}_R(\mathbf{w}_i^{n,-}, \mathbf{w}_i^{\star,+}) + \bar{\mathbf{w}}_L(\mathbf{w}_i^{\star,+}, \mathbf{w}_i^{n,+}) + \bar{\mathbf{w}}_R(\mathbf{w}_i^{\star,+}, \mathbf{w}_i^{n,+})\Big),$$

where

$$\bar{\mathbf{w}}_L(\mathbf{w}_L, \mathbf{w}_R) = \frac{\Delta t/2}{\Delta x/4} \int_{-\frac{\Delta x/4}{\Delta t/2}}^{0} \omega_e(\xi; \mathbf{w}_L, \mathbf{w}_R)\ d\xi,$$

$$= \mathbf{w}_L - \frac{\Delta t/2}{\Delta x/4}\left(\mathbf{f}(\omega_e(0;\mathbf{w}_L,\mathbf{w}_R)) - \mathbf{f}(\mathbf{w}_L)\right), \quad (12)$$

and

$$\bar{\mathbf{w}}_R(\mathbf{w}_L,\mathbf{w}_R) = \frac{\Delta t/2}{\Delta x/4}\int_0^{\frac{\Delta x/4}{\Delta t/2}} \omega_e(\xi;\mathbf{w}_L,\mathbf{w}_R)\, d\xi,$$
$$= \mathbf{w}_R - \frac{\Delta t/2}{\Delta x/4}\left(\mathbf{f}(\mathbf{w}_R) - \mathbf{f}(\omega_e(0;\mathbf{w}_L,\mathbf{w}_R))\right). \quad (13)$$

The function $\mathbf{f}$ refers to the exact flux function of the system (1) while $\omega_e(.;\mathbf{w}_L,\mathbf{w}_R)$ denotes the solution of the Riemann problem for (1) with the initial data $\mathbf{w}_0(x) = \mathbf{w}_L$ if $x < 0$ and $\mathbf{w}_R$ otherwise. An easy computation gives the following formula:

$$\mathbf{w}_i^{n+\frac{1}{2},+} = \left(\frac{1}{4}\mathbf{w}_i^{n,-} + \frac{1}{2}\mathbf{w}_i^{\star,+} + \frac{1}{4}\mathbf{w}_i^{n,+}\right) - \frac{\Delta t/2}{\Delta x}\left(\mathbf{f}(\mathbf{w}_i^{n,+}) - \mathbf{f}(\mathbf{w}_i^{n,-})\right).$$

Arguing the definition of $\mathbf{w}_i^{\star,+}$, given by (8), we have established that the integral formulation (11) coincides with the evolution step (3). Now, involving that $\mathbf{w}^h(x,\Delta t/2)$ belongs to the convex set Ω, the proof is achieved. □

To conclude the expected L[1]-stability result, we must satisfy the invariance of Ω during the last step of the MUSCL-Hancock method. To access such an issue, we propose to rewrite (4)-(5) as the average over the cell $(x_{i-\frac{1}{2}}, x_{i+\frac{1}{2}})$ of three values obtained by the first order scheme (6).

Following the ideas introduced in [2], let us introduce an intermediate state $\mathbf{w}_i^{n+\frac{1}{2},\star}$, uniquely defined as follows:

$$\frac{1}{4}\mathbf{w}_i^{n+\frac{1}{2},-} + \frac{1}{2}\mathbf{w}_i^{n+\frac{1}{2},\star} + \frac{1}{4}\mathbf{w}_i^{n+\frac{1}{2}.+} = \mathbf{w}_i^n. \quad (14)$$

The role played by the states $\mathbf{w}_i^{n+\frac{1}{2},\pm}$ and $\mathbf{w}_i^{n+\frac{1}{2},\star}$ is displayed in figure 2.

We propose to evolve each state using the associated first-order scheme (6) to obtain

$$\mathbf{w}_i^{n+1,-} = \mathbf{w}_i^{n+1\frac{1}{2},-} - \frac{\Delta t}{\Delta x/4}\left(\mathbf{f}(\mathbf{w}_i^{n+\frac{1}{2},-},\mathbf{w}_i^{n+\frac{1}{2},\star}) - \mathbf{f}(\mathbf{w}_{i-1}^{n+\frac{1}{2},+},\mathbf{w}_i^{n+\frac{1}{2},-})\right),$$

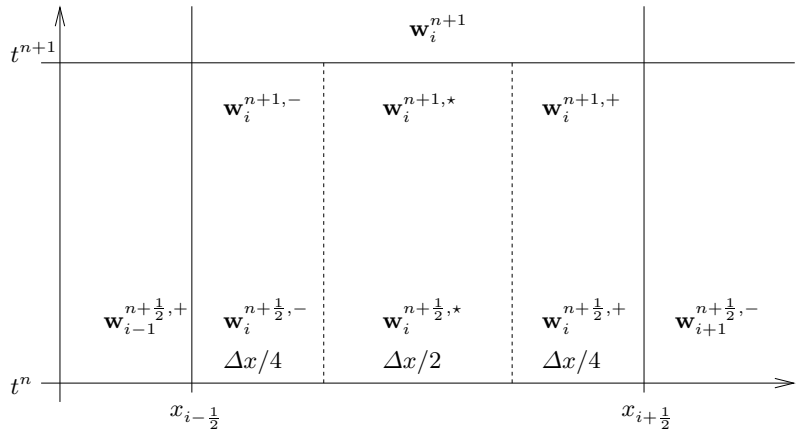

Fig. 2. Interpretation of the evolution step (4)-(5) as an average of values obtained by a first-order scheme

$$\mathbf{w}_i^{n+1,\star} = \mathbf{w}_i^{n+1\frac{1}{2},\star} - \frac{\Delta t}{\Delta x/2}\left(\mathbf{f}(\mathbf{w}_i^{n+\frac{1}{2},\star},\mathbf{w}_i^{n+\frac{1}{2},+}) - \mathbf{f}(\mathbf{w}_i^{n+\frac{1}{2},-},\mathbf{w}_i^{n+\frac{1}{2},\star})\right),$$
$$\mathbf{w}_i^{n+1,+} = \mathbf{w}_i^{n+1\frac{1}{2},+} - \frac{\Delta t}{\Delta x/4}\left(\mathbf{f}(\mathbf{w}_i^{n+\frac{1}{2},+},\mathbf{w}_{i+1}^{n+\frac{1}{2},-}) - \mathbf{f}(\mathbf{w}_i^{n+\frac{1}{2},\star},\mathbf{w}_i^{n+\frac{1}{2},+})\right).$$

We immediately deduce that the updated solution by (4)-(5) is nothing but the following average:

$$\mathbf{w}_i^{n+1} = \frac{1}{4}\mathbf{w}_i^{n+1,-} + \frac{1}{2}\mathbf{w}_i^{n+1,\star} + \frac{1}{2}\mathbf{w}_i^{n+1,+}. \tag{15}$$

Arguing this new formulation, we establish the expected numerical invariance of Ω during the step (4)-(5). Indeed, according with the first-order CFL restriction (7), assume the CFL like condition

$$\frac{\Delta t}{\Delta x/2}\max_{i\in\mathbb{Z}}\left(|\lambda_{i-1,i}^{+,-}|,|\lambda_{i,i}^{-,\star}|,|\lambda_{i,i}^{\star,+}|\right) \leq \frac{1}{2}, \tag{16}$$

where $\lambda_{i,j}^{+,-} = \lambda(\mathbf{w}_i^{n+\frac{1}{2},+},\mathbf{w}_j^{n+\frac{1}{2},-})$. As soon as the states $\mathbf{w}_i^{n+\frac{1}{2},\pm\star}$ belong to Ω for all $i\in\mathbb{Z}$, the L^1-stability property satisfied by the first-order scheme (6) implies that the states $\mathbf{w}_i^{n+1,\pm\star}$ are in Ω. Since Ω is a convex region, we deduce that $\mathbf{w}_i^{n+1}$, given by (15), belongs to Ω. We have established the following result:

Lemma 2 *Assume that the states* $(\mathbf{w}_i^{n+\frac{1}{2},\pm\star})_{i\in\mathbb{Z}}$ *belong to* Ω*, where* $\mathbf{w}_i^{n+\frac{1}{2},\star}$ *is given by (14). Assume the CFL restriction (16). The updated solution* $\mathbf{w}_i^{n+1}$*, given by (4)-(5), belongs to* Ω*.*

In the above result, let us note that we have imposed $\mathbf{w}_i^{n+\frac{1}{2},\pm\star} \in \Omega$ for all $i \in \mathbb{Z}$. Concerning $\mathbf{w}_i^{n+\frac{1}{2},\pm}$, it is a consequence of lemma 1. In fact, it is just necessary to establish a relevant condition to satisfy $\mathbf{w}_i^{n+\frac{1}{2},\star} \in \Omega$.

First, arguing the definition of $\mathbf{w}_i^{n+\frac{1}{2},\pm}$, given by (3), we deduce from (14) and the conservative reconstruction (2), the following formula:

$$\mathbf{w}_i^{n+\frac{1}{2},\star} = \mathbf{w}_i^n - \frac{\Delta t/2}{\Delta x}\left(\mathbf{f}(\mathbf{w}_i^{n,-}) - \mathbf{f}(\mathbf{w}_i^{n,+})\right).$$

We note that the above identity is very similar to the definition of $\mathbf{w}_i^{n+\frac{1}{2},\pm}$. As a consequence, lemma 1 can be easily extended to establish $\mathbf{w}_i^{n+\frac{1}{2},\star} \in \Omega$.

Lemma 3 *Assume that* $\mathbf{w}_i^n \in \Omega$ *for all* $i \in \mathbb{Z}$*. Let us define* $\mathbf{w}_i^{\star,\star}$ *as follows:*

$$\frac{1}{4}\mathbf{w}_i^{n,-} + \frac{1}{2}\mathbf{w}_i^{\star,\star} + \frac{1}{4}\mathbf{w}_i^{n,+} = \mathbf{w}_i^n. \tag{17}$$

Assume that $\mathbf{w}_i^{n,\pm}$ *and* $\mathbf{w}_i^{\star,\star}$ *are in* Ω*. Consider the following CFL condition:*

$$\frac{\Delta t/2}{\Delta x/4}\max_{i\in\mathbb{Z}}\left(|\lambda_e(\mathbf{w}_i^{\star,\star},\mathbf{w}_i^{n,-})|, |\lambda_e(\mathbf{w}_i^{n,+},\mathbf{w}_i^{\star,\star})|\right) \leq \frac{1}{2}, \tag{18}$$

then $\mathbf{w}_i^{n+\frac{1}{2},\star} \in \Omega$*.*

We omit the proof of this result which turns out to be the same as the proof of lemma 1.

With a conservative reconstruction, as proposed in (2), we note that (17) reads

$$\mathbf{w}_i^{\star,\star} = \mathbf{w}_i^n.$$

As a consequence, lemma 3 rewrite in the following simplified form:

Lemma 4 *Assume that* $\mathbf{w}_i^n \in \Omega$ *and* $\mathbf{w}_i^{n,\pm} \in \Omega$ *for all* $i \in \mathbb{Z}$*. Consider the CFL restriction*

$$\frac{\Delta t/2}{\Delta x/4}\max_{i\in\mathbb{Z}}\left(|\lambda_e(\mathbf{w}_i^{n},\mathbf{w}_i^{n,-})|, |\lambda_e(\mathbf{w}_i^{n,+},\mathbf{w}_i^{n})|\right) \leq \frac{1}{2}, \tag{19}$$

then $\mathbf{w}_i^{n+\frac{1}{2},\star} \in \Omega$*.*

From the above results, we deduce the expected stability property satisfied by the MUSCL-Hancock scheme (2)-(3)-(4)-(5):

Theorem 1 *Assume that* $\mathbf{w}_i^n \in \Omega$ *for all* $i \in \mathbb{Z}$. *Consider* $\mathbf{w}_i^{n,\pm}$, *defined by (2), and* $\mathbf{w}_i^{\star,\pm}$ *defined by (8). Assume that the slope* σ_i, *introduced in (2) to define the gradient reconstruction, satisfies*

$$\mathbf{w}_i^{\star,\pm} = \mathbf{w}_i^n \pm \Delta x \sigma_i \in \Omega. \tag{20}$$

Consider the CFL conditions (10)-(16)-(19). Then the updated solution $\mathbf{w}_i^{n+1}$, *defined by (2)-(3)-(4)-(5), is in* Ω.

Proof As soon as $\mathbf{w}_i^{n,\pm}$ belongs to Ω, we can apply lemma 1, lemma 2 and lemma 4 to obtain the result.

Now, we prove that $\mathbf{w}_i^{n,\pm}$ is in Ω. We note that

$$\mathbf{w}_i^{n,\pm} = \frac{1}{2}\mathbf{w}_i^{\star,\pm} + \frac{1}{2}\mathbf{w}_i^n.$$

Since $\mathbf{w}_i^{\star,\pm}$ and $\mathbf{w}_i^n$ are in Ω, the proof is completed when arguing the convex property of Ω. □

Currently, we have exhibit relevant CFL conditions and a slope limiter to ensure the L^1-stability of the MUSCL-Hancock numerical procedure. In the next section, extensions of the method are proposed. These variants will preserve the stability properties.

4 New variants

We consider two variants of the usual scheme (2)-(3)-(4)-(5). The first extension we consider, concerns the data reconstruction step. In (2), the gradient reconstruction is based on the conservative variables. Several authors recommend to consider other choice of variables; namely primitive or physical variables (for instance, see Karni [14]). We exhibit a suitable gradient reconstruction limitation in the case of non-conservative variables. The obtained numerical procedure preserves the L^1 stability property.

The second proposed variant concerns the time increment. From a practical point of view, the CFL restriction, given theorem 1, may involve difficulties to consider a time increment varying from an iteration to another. Indeed, the current CFL condition turns out to be *implicit*. The time increment Δt cannot be defined only considering $(\Delta x, \mathbf{w}_i^n)$ since the CFL conditions involve $\mathbf{w}_i^n$ and $\mathbf{w}_i^{n+\frac{1}{2}}$. We propose a new variant where Δt will be *explicit* and thus may vary easily from an iteration to another.

4.1 A non-conservative gradient reconstruction

In the data reconstruction step, we propose to introduce a linear-piecewise function based on a relevant change of variables. We set

$$\mathbf{U}^n(x) = \mathbf{U}_i^n + \sigma_i(x - x_i), \quad x \in (x_{i-\frac{1}{2}}, x_{i+\frac{1}{2}}),$$

with $\mathbf{U}_i^n = \kappa(\mathbf{w}_i^n)$ where κ denotes a smooth change of variable. The inner approximations, located at $x = x_{i\pm\frac{1}{2}}$, are given by

$$\mathbf{U}_i^{n,\pm} = \mathbf{U}_i^n \pm \frac{\Delta x}{2}\sigma_i, \tag{21}$$

to obtain the following reformulation of (2):

$$\begin{aligned} \mathbf{w}_i^{n,\pm} &= \kappa^{-1}(\mathbf{U}_i^{n,\pm}), \\ &= \mathbf{w}_i^{n,\pm} + \Delta\mathbf{w}_i^{n,\pm}. \end{aligned} \tag{22}$$

By opposition with the conservation approach, where we have set $\Delta\mathbf{w}_i^{n,\pm} = \pm\frac{\Delta x}{2}\sigma_i$, the non-conservative reconstruction is characterized by (see [2]):

$$\mathbf{w}_i^{n,-} + \mathbf{w}_i^{n,+} \neq 2\mathbf{w}_i^n.$$

Now, we consider the variant of the MUSCL-Hancock scheme defined by (22)-(3)-(4)-(5). To satisfy the L^1-stability property, we apply the same strategy as used in the section 3, enforcing the invariance of Ω at the end of each step.

First, the slope σ_i, introduced in (21), is limited in order to satisfy: $\mathbf{w}_i^{n,\pm} \in \Omega$ where $\mathbf{w}_i^{n,\pm}$ are defined by (22). Once again, let us note that this first limitation is standard. It enables to define $\mathbf{f}(\mathbf{w}_i^{n,\pm})$ in the second step.

Concerning the second step, lemma 1 can be applied to establish that $\mathbf{w}_i^{n+\frac{1}{2},\pm} \in \Omega$ but for $\mathbf{w}_i^{n+\frac{1}{2},\pm}$ defined by (22).

During the third step, lemma 2 remains true. In fact, the non-conservative form of the gradient reconstruction modifies the necessary condition to satisfy $\mathbf{w}_i^{n+\frac{1}{2},\star} \in \Omega$. Indeed, from (14), we deduce that $\mathbf{w}_i^{n+\frac{1}{2},\star}$ is now given by

$$\mathbf{w}_i^{n+\frac{1}{2},\star} = \left(2\mathbf{w}_i^n - \frac{\mathbf{w}_i^{n,-} + \mathbf{w}_i^{n,+}}{2}\right) - \frac{\Delta t/2}{\Delta x}\left(\mathbf{f}(\mathbf{w}_i^{n,-}) - v f(\mathbf{w}_i^{n,+})\right).$$

As a consequence, lemma 3 remains true but for the following definition of $\mathbf{w}_i^{\star,\star}$:

$$\frac{1}{4}\mathbf{w}_i^{n,-} + \frac{1}{2}\mathbf{w}_i^{\star,\star} + \frac{1}{4}\mathbf{w}_i^{n+1} = \left(2\mathbf{w}_i^n - \frac{\mathbf{w}_i^{n,-} + \mathbf{w}_i^{n,+}}{2}\right),$$

to obtain

$$\mathbf{w}_i^{\star,\star} = 4\mathbf{w}_i^n - 3\frac{\mathbf{w}_i^{n,-} + \mathbf{w}_i^{n,+}}{2}. \tag{23}$$

We conclude this presentation of the non-conservative reconstruction variant of the MUSCL-Hancock scheme, giving the following stability result:

Theorem 2 *Assume that* $\mathbf{w}_i^n \in \Omega$ *for all* $i \in \mathbb{Z}$*.Consider* $\mathbf{w}_i^{n,\pm}$ *defined by (22),* $\mathbf{w}_i^{\star,\pm}$ *defined by (8) and* $\mathbf{w}_i^{\star,\star}$ *defined by (23). Assume that the slope* σ_i *satisfies*

$$\mathbf{w}_i^{n\pm} \in \Omega, \quad \mathbf{w}_i^{\star,\pm} \in \Omega \quad \textit{and} \quad \mathbf{w}_i^{\star,\star} \in \Omega. \tag{24}$$

Consider the CFL conditions (10)-(16)-(18). Then, the updated state $\mathbf{w}_i^{n+1}$*, given by (22)-(3)-(4)-(5), belongs to* Ω*.*

4.2 Varying time increments

Both conservative and non-conservative variant of the MUSCL-Hancock method involve the same difficulties when evaluating the time increment Δt. From a practical point of view, numerical simulations recommend that Δt may vary from an iteration to another. Currently, this is not possible in the framework of theorem 1 or theorem 2 where the CFL condition seems to be *implicit*. Indeed, to compute Δt, the knowledge of Δx, $\mathbf{w}_i^n$ but also $\mathbf{w}_i^{n+\frac{1}{2}}$ are necessary where $\mathbf{w}_i^{n+\frac{1}{2}}$ depends on Δt. To suppress this difficulty when evaluating Δt, we propose a new variant of the numerical procedure where the time increment will be explicitly known at the end of each step of the scheme. To access such an issue, we propose to consider two independent time step Δt_1 and Δt_2 respectively associated with (3) and (4)-(5).

For the sake of simplicity, we detail this new variant in the case of conservative data reconstruction. We propose the following numerical procedure to substitute to (3) and (4):

$$\begin{cases} \mathbf{w}_i^{n+\frac{1}{2},\pm} = \mathbf{w}_i^{n,\pm} - \dfrac{\Delta t_1/2}{\Delta x}\left(\mathbf{f}(\mathbf{w}_i^{n,+}) - \mathbf{f}(\mathbf{w}_i^{n,-})\right), \\ \bar{\mathbf{w}}_i = \dfrac{1}{2}\left(\mathbf{w}_i^{n+\frac{1}{2},-} + \mathbf{w}_i^{n+\frac{1}{2},+}\right), \\ \bar{\bar{\mathbf{w}}}_i = \mathbf{w}_i^n - \dfrac{\Delta t_2}{\Delta x}\left(\mathbf{f}_{i+\frac{1}{2}} - \mathbf{f}_{i-\frac{1}{2}}\right), \\ \mathbf{w}_i^{n+1} = \alpha\bar{\bar{\mathbf{w}}}_i + (1-\alpha)\bar{\mathbf{w}}_i, \end{cases} \tag{25}$$

where α is given by

$$\alpha = \begin{cases} \Delta t_1 \frac{\Delta t_1 - 2\sqrt{\Delta t_2(\Delta t_1 - \Delta t2)}}{(\Delta t_1 - \Delta t_2)^2}, & \text{if } \Delta t_2 < \Delta t_1, \\ \frac{1}{2}, & \text{if } \Delta t_2 = \Delta t_1. \end{cases}$$

Now, the updated solution $\mathbf{w}_i^{n+1}$ is given for a time $t^n + \Delta t$ where Δt is defined as follows:

$$\Delta t = \alpha \Delta t_2 + (1 - \alpha)\frac{\Delta t_1}{2}.$$

This scheme is easily seen to be second-order of accuracy. In addition, we note that the standard MUSCL-Hancock scheme, detailed in section 2, coincides with the fixed choice $\Delta t_1 = \Delta t_2 = \Delta t$.

We turn considering the stability of this method. We see that lemma 1 can be applied to ensure that the states $\mathbf{w}_i^{n+\frac{1}{2},\pm}$ belong to Ω as soon as Δt_1 satisfies the CFL restriction (10). Similarly, we have $\mathbf{w}_i^{n+\frac{1}{2},\star}$ in Ω if Δt_1 satisfy the CFL like condition (19) (see lemma 4). From lemma 2, we deduce that $\bar{\bar{\mathbf{w}}}_i$ belongs to Ω if the CFL condition (16), applied to Δt_2, is satisfied. Arguing the convex property of Ω, we immediately obtain that $\bar{\mathbf{w}}_i$ and next $\mathbf{w}_i^{n+1}$ are in Ω.

To conclude, let us emphasize that the CFL conditions (10) and (19), used to restrict Δt_1, only involve $\mathbf{w}_i^n$ and $\mathbf{w}_i^{n,\pm}$. Then, $\mathbf{w}_i^{n+\frac{1}{2},\pm}$ and $\mathbf{w}_i^{n+\frac{1}{2},\star}$ can be evaluated. Next, the time increment Δt_2 is restrict when considering the CFL condition (10) based on $\mathbf{w}_i^{n+\frac{1}{2}}$. In this sense, the time increment computations are *explicit* when considering this new extension of the initial scheme.

5 Numerical experiments

In this section, we perform several numerical tests using the MUSCL-Hancock procedure we have investigated. These experiments are performed when approximating the solutions of Euler equations:

$$\begin{cases} \partial_t \rho + \partial_x \rho u = 0, \\ \partial_t \rho u + \partial_x (\rho u^2 + p) = 0, \\ \partial_t E + \partial_x (E + p) u = 0, \end{cases} \tag{26}$$

where the pressure is given by the perfect gas law:

$$p = (\gamma - 1)\left(E - \rho \frac{u^2}{2}\right), \quad \gamma \in (1, 3].$$

The set Ω of the admissible states is defined as follows:

$$\Omega = \left\{ \mathbf{w} \in \mathbb{R}^3;\ \rho > 0, u \in \mathbb{R}, e(\mathbf{w}) = E - \rho\frac{u^2}{2} > 0 \right\}.$$

In the sequel, the variables $\mathbf{w} = (\rho, \rho u, E)$ are denoted the conservative variables while $\mathbf{U} = (\rho, u, p)$ will denote the non-conservative primitive variables.

In the present work, the numerical flux function, used in (5), is based on the Suliciu relaxation scheme (see Jin-Xin [13], but also [1,3,5,7] to several derivations). To conclude the presentation of the scheme, we have to describe the limitation used within the gradient reconstruction. We propose to extend the standard limitation procedures (minmod, superbee, etc., see [18,24] and references therein) to enforce the additional restriction stated in theorem 1 (for a conservative reconstruction) or theorem 2 (for a non-conservative reconstruction).

First, let us consider the conservative gradient reconstruction. In view of the definition (2), we search for a gradient reconstruction in the form

$$\begin{cases} \rho_i^{n,\pm} = \rho_i^n \pm \Delta\rho, \\ (\rho u)_i^{n,\pm} = (\rho u)_i^n \pm \Delta\rho u, \\ E_i^{n,\pm} = E_i^n \pm \Delta E, \end{cases}$$

where the increment $\Delta\mathbf{w} = (\Delta\rho, \Delta\rho u, \Delta E)$ must satisfy the stability condition (20) which reads:

$$\rho_i^n \pm 2\Delta\rho > 0, \tag{27}$$

$$(E_i^n \pm 2\Delta E) - \frac{\left((\rho u)_i^n \pm 2\Delta\rho u\right)^2}{2(\rho_i^n \pm 2\Delta\rho)} > 0. \tag{28}$$

The condition (27) writes:

$$\left| \frac{2\Delta\rho}{\rho_i^n} \right| < 1. \tag{29}$$

Concerning the inequalities (28), it appears a compatibility condition. Indeed, the sum of the two equalities involved in (28) gives:

$$2E_i^n - \left(\frac{\left((\rho u)_i^n + 2\Delta\rho u\right)^2}{2(\rho_i^n + 2\Delta\rho)} + \frac{\left((\rho u)_i^n - 2\Delta\rho u\right)^2}{2(\rho_i^n - 2\Delta\rho)} \right) > 0. \tag{30}$$

As a consequence, we have to find a pair $(\Delta\rho, \Delta\rho u)$ which satisfies the above inequality. To access such an issue, momentarily we propose to

fix $\Delta\rho u = 0$ and to exhibit a relevant $\Delta\rho$. Next, $\Delta\rho$ is plugged into (30) and $\Delta\rho u$ is evaluated. We propose to consider $\Delta\rho$ such that

$$2E_i^n - \left(\frac{((\rho u)_i^n)^2}{2(\rho_i^n + 2\Delta\rho)} + \frac{((\rho u)_i^n)^2}{2(\rho_i^n - 2\Delta\rho)} \right) > 0, \tag{31}$$

which coincides with (30) but for $\Delta\rho u = 0$. From (31), we deduce

$$\left| \frac{2\Delta\rho}{\rho_i^n} \right| < \sqrt{\frac{E_i^n - \rho_i^n \frac{(u_i^n)^2}{2}}{E_i^n}} < 1. \tag{32}$$

We use (32) to fix $\Delta\rho$. Next, with the fixed $\Delta\rho$, the inequality (30) gives a relevant choice of $\Delta\rho u$. Finally, the increment ΔE is considered to satisfy (28). We obtain the following modified gradient reconstruction:

$$\Delta\rho = \max\left(-\frac{\rho_i^n}{2}\sqrt{\frac{E_i^n - \rho_i^n \frac{(u_i^n)^2}{2}}{E_i^n}}, \min\left(\frac{\rho_i^n}{2}\sqrt{\frac{E_i^n - \rho_i^n \frac{(u_i^n)^2}{2}}{E_i^n}}, \frac{\Delta x}{2}\sigma_i^\rho \right) \right), \tag{33a}$$

$$\Delta\rho u = \max\left(\xi^-, \min\left(\xi^+, \frac{\Delta x}{2}\sigma_i^{\rho u} \right) \right), \tag{33b}$$

$$\Delta E = \max\left(-\frac{1}{2}\left(E_i^n - \frac{((\rho u)_i^n + 2\Delta\rho u)^2}{2(\rho_i^n + 2\Delta\rho)} \right), \min\left(\frac{1}{2}\left(E_i^n - \frac{((\rho u)_i^n - 2\Delta\rho u)^2}{2(\rho_i^n - 2\Delta\rho)} \right), \frac{\Delta x}{2}\sigma_i^E \right) \right), \tag{33c}$$

where

$$\xi^\pm = \frac{1}{2}u_i^n \Delta\rho \pm \frac{1}{2}\sqrt{2\left(\rho_i^n - \frac{4\Delta\rho^2}{\rho_i^n}\right)\left(E_i^n - \rho_i^n \frac{(u_i^n)^2}{2}\right)}.$$

The numerical experiments will assert the interest of the procedure.

Now, we turn considering the non-conservative reconstruction approach. We search for a gradient reconstruction in the form:

$$\begin{cases} \rho_i^{n,\pm} = \rho_i^n \pm \Delta\rho, \\ u_i^{n,\pm} = u_i^n \pm \Delta u, \\ p_i^{n,\pm} = p_i^n \pm \Delta p, \end{cases}$$

where the increment $(\Delta\rho, \Delta u, \Delta p)$ must satisfy the stability condition (24). After computations, this restriction reads:

$$\rho_i^n \pm \Delta\rho, \quad \rho_i^n \pm 2\Delta\rho > 0, \tag{34}$$

$$p_i^n \pm \Delta p > 0, \tag{35}$$

$$p_i^{\star,\pm} = p_i^n \pm 2\Delta p - \frac{3}{2}(\gamma-1)\frac{\Delta u^2}{\rho_i^n \pm 2\Delta\rho}\left((\rho_i^n)^2 - \Delta\rho^2\right) > 0, \tag{36}$$

$$p_i^{\star,\star} = p_i^n - \frac{3}{2}(\gamma-1)\frac{\Delta u^2}{\rho_i^n}\left((\rho_i^n)^2 + 3\Delta\rho^2\right) > 0. \tag{37}$$

We note that the inequalities $p_i^{\star,+} > 0$ and $p_i^{\star,-} > 0$ involve a compatibility condition. Indeed, the increments must satisfy $p_i^{\star,+} + p_i^{\star,-} > 0$ which writes:

$$p_i^n - \frac{3}{2}(\gamma-1)\Delta u^2 \frac{\rho_i^n}{(\rho_i^n - 2\Delta\rho)(\rho_i^n + 2\Delta\rho)} > 0. \tag{38}$$

It is easy to check that (38) is more restrictive than $p_i^{\star,\star} > 0$. As a consequence, we only consider (38) instead of $p_i^{\star,\star} > 0$.

First, we determine the pair $(\Delta\rho, \Delta u)$ such that the above inequality (38) is satisfied. We propose to consider Δu such that

$$p_i^n - \frac{3}{2}(\gamma-1)\Delta u^2 \rho_i^n > 0, \tag{39}$$

which coincides with (38) but for $\Delta\rho = 0$. We obtain

$$|\Delta u| < \sqrt{\frac{p_i^n}{\frac{3}{2}(\gamma-1)\rho_i^n}}. \tag{40}$$

We fix Δu according to (40) and we consider $\Delta\rho$ to satisfy (38):

$$\left|\frac{\Delta\rho}{\rho_i^n}\right| < \sqrt{\frac{\frac{p_i^n}{\frac{3}{2}(\gamma-1)\rho_i^n\Delta u^2} - 1}{4\frac{p_i^n}{\frac{3}{2}(\gamma-1)\rho_i^n\Delta u^2} - 1}} < \frac{1}{2}. \tag{41}$$

The increment Δp is thus considered to satisfy (36).

Finally, the gradient reconstruction is modified as follows:

$$\Delta u = \max\left(-\frac{p_i^n}{\frac{3}{2}(\gamma-1)\rho_i^n}, \min\left(\frac{p_i^n}{\frac{3}{2}(\gamma-1)\rho_i^n}, \frac{\Delta x}{2}\sigma_i^u\right)\right), \tag{42a}$$

$$\Delta\rho = \max\left(-\rho\sqrt{\frac{\frac{p_i^n}{\frac{3}{2}(\gamma-1)\rho_i^n} - \Delta u^2}{4\frac{p_i^n}{\frac{3}{2}(\gamma-1)\rho_i^n} - \Delta u^2}},\right.$$

$$\min\left(\rho\sqrt{\frac{\frac{p_i^n}{\frac{3}{2}(\gamma-1)\rho_i^n}-\Delta u^2}{4\frac{p_i^n}{\frac{3}{2}(\gamma-1)\rho_i^n}-\Delta u^2}},\frac{\Delta x}{2}\sigma_i^\rho\right)\right), \tag{42b}$$

$$\Delta p=\max\left(-\frac{1}{2}\left(p_i^n-\frac{3}{2}(\gamma-1)\frac{\Delta u^2}{\rho_i^n+2\Delta\rho}((\rho_i^n)^2-\Delta\rho^2)\right),\right.$$
$$\left.\min\left(\frac{1}{2}\left(p_i^n-\frac{3}{2}(\gamma-1)\frac{\Delta u^2}{\rho_i^n-2\Delta\rho}((\rho_i^n)^2-\Delta\rho^2)\right),\frac{\Delta x}{2}\sigma_i^p\right)\right). \tag{42c}$$

Now, we illustrate the numerical procedure with several tests. They are performed using the same strategy. The mesh is assumed to be uniform and made of 100 cells. Concerning the computation of the slope σ_i (see (2)), we propose to consider the minmod and the superbee function (see [18] to further details). These limitations are modified according to (33) or (42). The numerical results are systematically compared with the exact solution.

The first test is devoted to confirm the second-order of accuracy of the method. We propose to consider the following smooth initial data: $u(x,0)=1$, $p(x,0)=1$ and

$$\rho(x,0)=\begin{cases}100 & \text{if } x<-0.4,\\ 100(2-\cos(3x+1.2)^2) & \text{otherwise.}\end{cases}$$

The gradient reconstruction uses the non-conservative approach (42) where the slope σ_i is defined by the superbee function (see [18]). In the following table we give the numerical order of accuracy obtained for the variable ρ at time $t=0.1$. This numerical order is computed from a run with 50 cells to another run.

cells	modified	standard
100	1.99	2.03
200	2.00	2.02
500	1.95	1.96
800	1.82	1.84

We have compared the modified superbee limitation according to (42) and the standard superbee limiter [18].

The next test corresponds to a Riemann solution made of a shock wave and a rarefaction wave separated by a contact discontinuity. The initial data is made of two constant states defined as follows:

$$\rho_L=2 \qquad u_L=0\ p_L=100$$
$$\rho_R=0.125\ u_R=0\ p_R=0.1$$

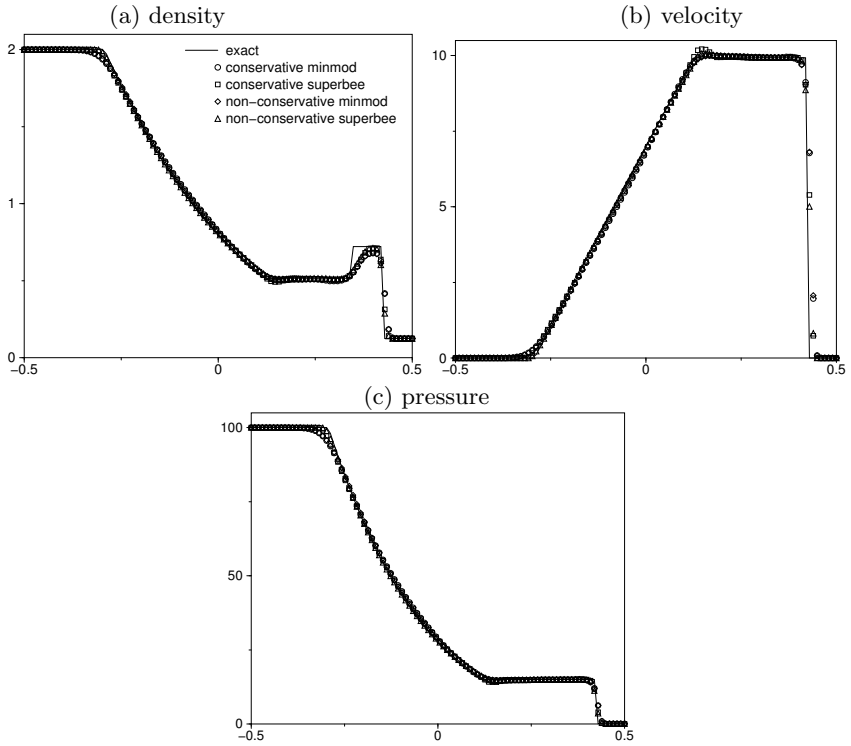

Fig. 3. Shock tube problem: exact solution (fill line), conservative reconstruction based on the minmod function (∘ symbol), conservative reconstruction based on the superbee function (□ symbol), non-conservative reconstruction based on the minmod function (◇ symbol), non-conservative reconstruction based on the superbee function (△ symbol).

The left and right states are separated by a discontinuity located at $x = 0$. The solution is displayed at the time $t = 0.035$. The numerical results are displayed in figure 3. The considered gradient reconstruction is defined from conservative (33) and non-conservative (42) variables. The minmod function and the superbee function (see [18]) are considered to define the slope σ_i. We report the numerical order of accuracy computed by comparison between two runs with different mesh size. The first run is fixed with 50 cells. The first following table shows the numerical order of accuracy obtained with the minmod function based on conservative variables. In the second table, the order of accuracy is given when considering the non-conservative reconstruction based on the superbee function.

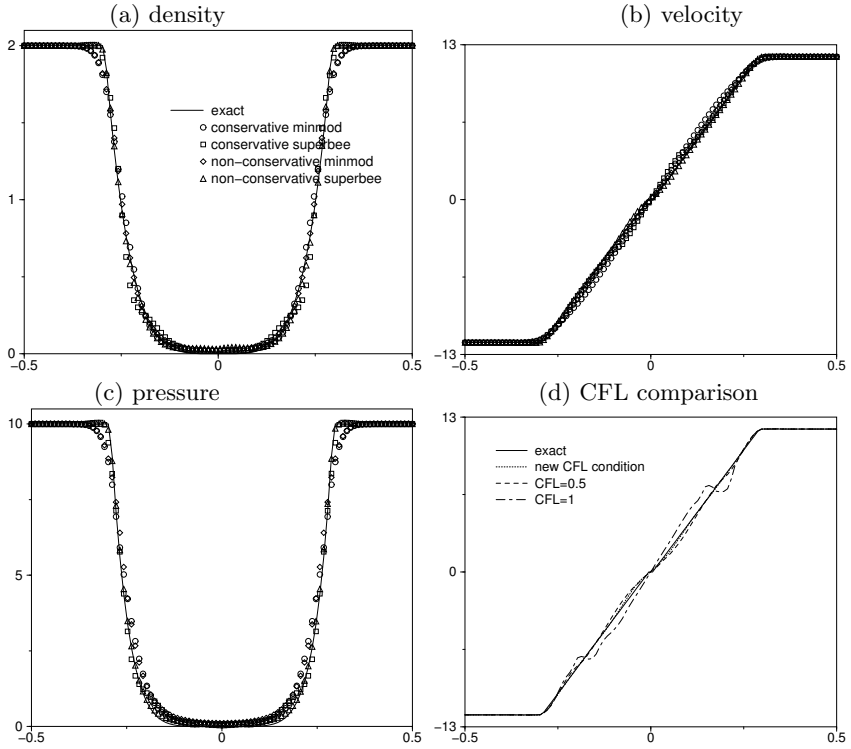

Fig. 4. Two rarefaction waves problem. Graphs (a)-(b)-(c): exact solution (fill line), conservative reconstruction based on the minmod function (∘ symbol), conservative reconstruction based on the superbee function (□ symbol), non-conservative reconstruction based on the minmod function (◇ symbol), non-conservative reconstruction based on the superbee function (△ symbol). Graph (d): varying CFL number with a non-conservative reconstruction based on the superbee function.

conservative minmod

cells	ρ	u	p
100	0.94	1.20	0.99
200	0.95	1.10	0.99
500	0.93	1.04	0.99
800	0.92	1.02	0.99

non-conservative superbee

cells	ρ	u	p
100	0.93	1.14	1.04
200	0.94	1.06	1.02
500	0.91	1.01	1.01
800	0.92	0.99	1.00

In the third test, we consider a Riemann solution made of two rarefaction waves. The left and right states which made the initial data are defined as follows:

$$\rho_L = 2 \; u_L = -12 \; p_L = 10$$
$$\rho_R = 2 \; u_R = 12 \quad p_R = 10$$

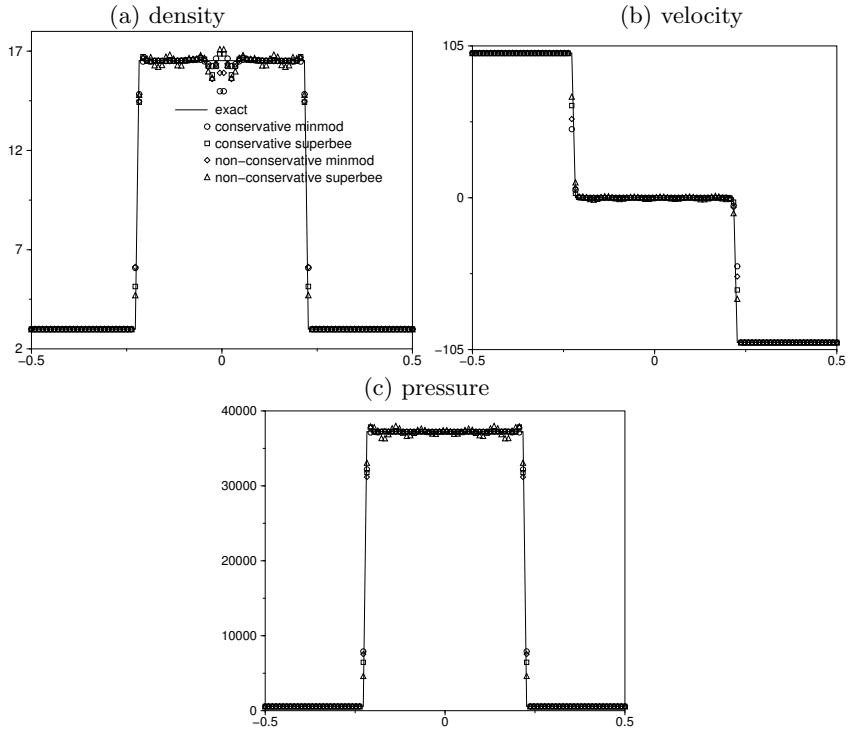

Fig. 5. Two shock waves problem: exact solution (fill line), conservative reconstruction based on the minmod function (○ symbol), conservative reconstruction based on the superbee function (□ symbol), non-conservative reconstruction based on the minmod function (◇ symbol), non-conservative reconstruction based on the superbee function (△ symbol).

The solution is displayed at the time $t = 0.02$ in figure 4. In addition, figure 4 displays the numerical velocity obtained when involving several choices of the CFL number. For a CFL number equal to 0.5, we observe very small oscillations. These oscillations clearly increase for a CFL number equal to 1.

The last test concerns a Riemann solution made of two shock waves. The initial data for this test is defined as follows:

$$\rho_L = 3 \; u_L = 100 \quad p_L = 573$$
$$\rho_R = 3 \; u_R = -100 \; p_R = 573$$

The numerical solutions are displayed at the time $t = 0.01$ in figures 5.

The two last experiments are known to be very difficult. When performing these two tests, the method is shown to be robust according to theorem 1 or theorem 2. However, concerning the two shock

waves problem, we observe a spike in the 2-contact discontinuity for the density. Let us note that this spike is standard and it can be observed within the first-order relaxation scheme or Roe scheme or Osher scheme (for instance). It appears when approximating shocks resulting from two opposing hypersonic flows (see Liska-Wendroff [19] or Noh [21]). This difficulty is preserved in the present work and it induces oscillations when considering a second-order MUSCL Hancock scheme.

Acknowledgements The author thanks P. Helluy to initiate this work during the conference *Numerical Simulation of Complex and Multiphase Flows*.

References

1. M. Baudin, C. Berthon, F. Coquel, R. Masson, H. Tran, *A relaxation method for two-phase flow models with hydrodynamic closure law*, Numer. Math. 99, no 3, pp. 411–440 (2005).
2. C. Berthon, *Stability of the MUSCL schemes for the Euler equations*, Comm. Math. Sci. 3, pp. 133–158 (2005).
3. C. Berthon, *Numerical approximations of the 10-moment Gaussian closure*, Math. Comp., accepted.
4. F. Bianco, G. Puppo, G. Russo, *High-order central schemes for hyperbolic systems of conservation laws*, SIAM J. Sci. Comput. 21, no. 1, pp. 294-322 (1999)
5. F. Bouchut, *Nonlinear stability of finite volume methods for hyperbolic conservation laws, and well-balanced schemes for sources*, Frontiers in Mathematics series, Birkhäuser (2004).
6. P. Colella, *Multidimensional upwind methods for hyperbolic conservation laws*, J. Comput. Phys. 87, pp. 171-200 (1990).
7. F. Coquel, B. Perthame, *Relaxation of energy and approximate Riemann solvers for general pressure laws in fluid dynamics*, SIAM J. Numer. Anal. 35, no. 6, pp. 2223-2249 (1998).
8. S. Cordier, C. Buet, *Asymptotic preserving scheme for radiative hydrodynamics model*, preprint.
9. L. J. Durlofsky, B. Engquist, S. Osher, *Triangle based adaptive stencils for the solution of hyperbolic conservation laws*, J. Comput. Phys. 98, pp. 64-73 (1992).
10. E. Godlewski, P.A. Raviart, *Hyperbolic systems of conservations laws*, SMAI (Eds), Ellipse (1991).
11. E. Godlewski, P.A. Raviart, *Hyperbolic systems of conservations laws*, Applied Mathematical Sciences, Vol 118, Springer (1995).
12. A. Harten, P.D. Lax, B. Van Leer, *On upstream differencing and Godunov-type schemes for hyperbolic conservation laws*, SIAM Review, Vol 25, No 1, pp. 35-61 (1983).
13. S. Jin, Z. Xin, *The Relaxation Scheme for Systems of Conservation Laws in Arbitrary Space Dimension*, Comm. Pure Appl. Math., **45**, 235–276 (1995).
14. S. Karni, *A multicomponent flow calculations by a consistent primitive algorithm*, J. Comp. Phys. 112, pp. 31–43 (1994).

15. B. Khobalatte, B. Perthame, *Maximum principle on the entropy and second-order kinetic schemes*, Math. of Comp., Vol 62, No 205, pp. 119-131 (1994).
16. B. van Leer, *Towards the ultimate conservative difference scheme. V. A second-order sequel to Godunov's method*, J. Comput. Phys. 32, pp. 101-136 (1979).
17. B. van Leer, *On the relation between the upwind-differencing schemes of Godunov, Engquist-Osher and Roe*, SIAM J. Sci. Statist. Comput. 5, No. 1, pp. 1-20 (1984).
18. R. J. LeVeque, *Finite volume methods for hyperbolic problems*, Cambridge Texts in Applied Mathematics. Cambridge University Press, Cambridge (2002).
19. R. Liska and B. Wendroff, *Comparison of several difference schemes on 1D and 2D test problems for the Euler equations*, SIAM J. Sci. Comput., 25, No.3, 995–1017 (2003).
20. H. Nessyahu, E. Tadmor, *Nonoscillatory central differencing for hyperbolic conservation laws*, J. Comput. Phys. 87, no. 2, pp. 408-463 (1990).
21. W.F. Noh, *Errors for calculations of strong shocks using an artificial viscosity and an artificial heat flux*, J. Comput. Phys., 72, 78–120 (1987).
22. B. Perthame, Y. Qiu, *A variant of Van Leer's method for multidimensional systems of conservation laws*, J. Comput. Phys. 112, no. 2, 370–381 (1994).
23. R. Sanders, A. Weiser, *High resolution staggered mesh approach for nonlinear hyperbolic systems of conservation laws*, J. Comput. Phys. 101, pp. 314-329 (1992).
24. E. F. Toro, *Riemann solvers and numerical methods for fluid dynamics. A practical introduction* Second edition. Springer-Verlag, Berlin (1999).